© 2015. Published by The Company of Biologists Ltd | Journal of Cell Science (2015) 128, 219–224 doi:10.1242/jcs.142463

SHORT REPORT

Skeletal muscle intermediate filaments form a stress-transmitting and stress-signaling network

Michelle G. Palmisano[1], Shannon N. Bremner[1], Troy A. Hornberger[2], Gretchen A. Meyer[1], Andrea A. Domenighetti[1], Sameer B. Shah[3], Balázs Kiss[4], Miklos Kellermayer[4], Allen F. Ryan[5] and Richard L. Lieber[1,*]

ABSTRACT

A fundamental requirement of cells is their ability to transduce and interpret their mechanical environment. This ability contributes to regulation of growth, differentiation and adaptation in many cell types. The intermediate filament (IF) system not only provides passive structural support to the cell, but recent evidence points to IF involvement in active biological processes such as signaling, mechanotransduction and gene regulation. However, the mechanisms that underlie these processes are not well known. Skeletal muscle cells provide a convenient system to understand IF function because the major muscle-specific IF, desmin, is expressed in high abundance and is highly organized. Here, we show that desmin plays both structural and regulatory roles in muscle cells by demonstrating that desmin is required for the maintenance of myofibrillar alignment, nuclear deformation, stress production and JNK-mediated stress sensing. Finite element modeling of the muscle IF system suggests that desmin immediately below the sarcolemma is the most functionally significant. This demonstration of biomechanical integration by the desmin IF system suggests that it plays an active biological role in muscle in addition to its accepted structural role.

KEY WORDS: Biomechanics, Desmin, Mechanotransduction, Tensegrity

INTRODUCTION

A fundamental requirement for cells is the ability to transduce and interpret their mechanical environment (Buxboim et al., 2010; Engler et al., 2006). Several systems have been identified that accomplish this task including members of the G-protein family that transduce membrane shear stress (Frangos et al., 1988), integrin receptors that sense cell surface tension through ligand binding (Ruoslahti and Pierschbacher, 1987), and strain-activated ion channels that alter conductance when deformed (Guharay and Sachs, 1984). In addition, it has been proposed that the cellular cytoskeleton provides a network through which the mechanical state can be transduced by microfilaments, microtubules and/or intermediate filaments (IFs) to induce protein conformational change and nuclear deformation that can alter biological activity (Maniotis et al., 1997; Sawada et al., 2006). IF disruption specifically leads to a number of diseases (Fuchs and Cleveland, 1998; Traub and Shoeman, 1994), implying a crucial biological role. However, the mechanism by which IFs might exert biological activity and how they might interact with the muscle fiber cellular machinery are not clear (Herrmann et al., 2007).

A powerful system in which to address IF function is skeletal muscle, which expresses desmin, a tissue-specific type III IF. Previous studies have shown that desmin is localized specifically to the skeletal muscle Z-disk, where it interconnects myofibrils laterally and, to a lesser extent, longitudinally (Wang and Ramirez-Mitchell, 1983). Based primarily on these localization data, as well as the deranged structure and function of myofibrils in desmin-null muscles, desmin has been proposed to be a primary mechanical integrator of the muscle fiber (Lazarides, 1980) being strategically located to maintain sarcomere alignment and homogeneity (Morgan, 1990). In addition to this proposed mechanical role, a biological role for desmin is suggested by the fact that it is one of the first muscle-specific genes that is expressed during development (Rudnicki et al., 1993) and is found in high concentration around subcellular organelles such as nuclei and mitochondria (Milner et al., 2000). Although indirect, this evidence suggests a potential role for desmin as a mechanical force transmitter and spatial organizer.

To better define the role(s) of desmin, DNA encoding a GFP–desmin fusion protein was introduced into adult muscles lacking desmin. This has allowed us to distinguish the functional role of desmin in adult muscle from the developmental consequences of desmin deficiency and to more directly link desmin to events that occur in muscle when it is activated or deformed.

RESULTS AND DISCUSSION

As expected, wild-type (WT) muscle showed high sarcomere matrix regularity and continuity under strain (Fig. 1A–A″), whereas desmin-null muscles showed irregular sarcomeres and loss of spatial continuity (Fig. 1B–B″). Single fibers microdissected from transfected mutant muscles showed regional GFP–desmin expression (Fig. 1C) and confocal microscopy of these transfected areas showed realigned myofibrils and restored spatial continuity during loading, demonstrating mechanically functional connections (Fig. 1D–D″). The displacement of adjacent myofibrillar Z-disks was quantified by Fourier analysis (Shah and Lieber, 2003) and expressed as the phase-shift variance between adjacent myofibrils under stretch (Fig. 1E; Shah et al.,

[1]Departments of Orthopaedics, Bioengineering, Medicine and the Biomedical Sciences Graduate Group, University of California and Veterans Administration Medical Centers, San Diego, CA 92093, USA. [2]Department of Comparative Biology, University of Wisconsin, Madison, WI 53706, USA. [3]Fischell Department of Bioengineering, University of Maryland, College Park, MD 20742, USA. [4]MTA-SE Molecular Biophysics Research Group, Department and Radiation Biology, Semmelweis, University, Budapest 1094, Hungary. [5]Department of Otolaryngology, University of California and Veterans Administration Medical Centers, San Diego, CA 92161, USA.

*Author for correspondence (rlieber@ucsd.edu)

Received 30 October 2013; Accepted 1 November 2014

Journal of Cell Science

Journal of Cell Science (2015) 128, 219–224 doi:10.1242/jcs.142463

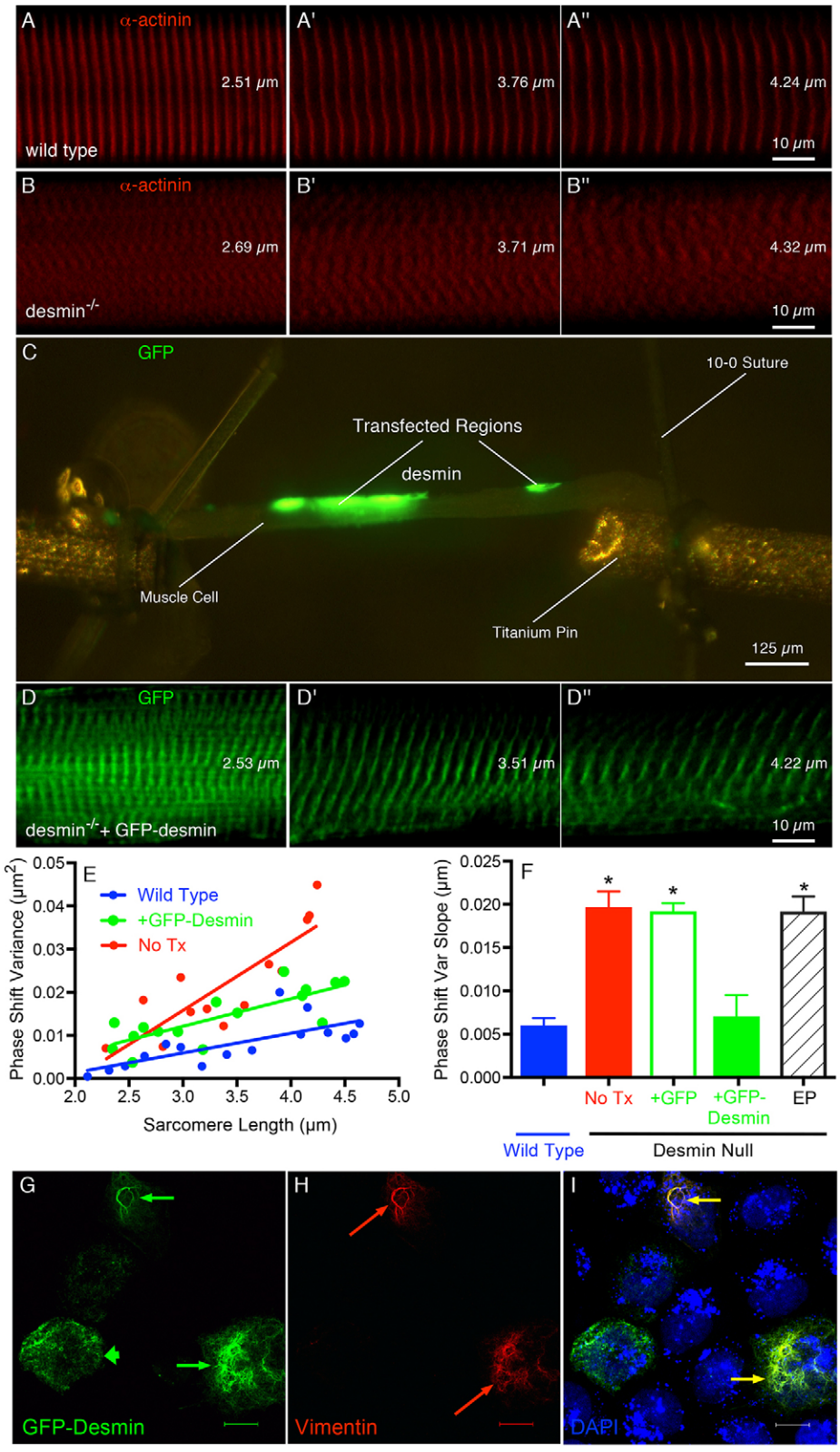

Fig. 1. Reintroduction of GFP–desmin rescues the normal striation pattern in desmin-null muscles. Serial confocal images of the Z-disk striations in single muscle cells being stretched while imaging the striation pattern as described previously (Shah and Lieber, 2003). (A,B,D) These panels represent three different cells at three comparable sarcomere lengths (shown on each image). (C) A low-power image of the single cell mounted between titanium pins in the *in vitro* testing chamber showing the two transfected regions in green. (A–A″) WT muscle cell. (B–B″) Desmin-null muscle cell. (D–D″) Desmin-null muscle cell transfected with GFP–desmin and imaged in a transfected region (region highlighted in C). All cells are also labeled with α-actinin except the desmin-null muscle cell transfected with GFP–desmin. (E) Sample myofibrillar phase-shift variance values as a function of sarcomere length obtained from each of the experimental groups. Note the similarity in slopes between the WT (0.00456 μm^2) and the transfected desmin-null muscles (+GFP-desmin, 0.00639 μm^2) compared to the desmin-null muscle, which is about three times greater (No Tx, 0.0158 μm^2). (F) Quantification of the degree of 'connectivity' across the fiber as the phase-shift slope of the striation pattern, which is obtained as the fiber is stretched (Shah et al., 2004). The two treatments with the greatest connectivity are the WT and desmin-null muscle transfected with GFP–desmin, which are both significantly different to the other three treatment groups. *$P<0.0001$ (Student's *t*-test). Data represent mean±s.e.m., for $n=5$–8 muscles/group. (G–I) Confocal images of three SW13 cells transfected with the GFP–desmin construct used in the muscle experiments. (G) GFP–desmin expression is strong in all three cells but two demonstrate extended IF networks (thin arrows) whereas one demonstrates more punctate expression (thick arrow). (H) Vimentin expression and filament formation is robust in two of the three cells (red arrows). (I) Overlay of GFP–desmin and vimentin channels showing extended IF networks only when vimentin is also expressed (yellow arrows). Scale bar: 15 μm.

2004). The slope of this relationship indicates the degree of connectivity among myofibrils. The phase-shift variance slope was not significantly different between WT and GFP–desmin-transfected desmin-null muscles (Fig. 1F, +GFP–desmin, $P>0.7$), but both were significantly lower than that found for the desmin-null muscle (No Tx; Fig. 1F), desmin-null muscles transfected with GFP alone (Fig. 1F, +GFP) or desmin-null muscles subjected to electroporation alone (Fig. 1F, EP, $P<0.001$). Thus, the properties of muscle that differ in desmin-null mice are attributable to desmin, not to the indirect effect of lack of desmin during development or to the transfection procedure because only GFP–desmin realigned myofibrils. Interestingly,

Journal of Cell Science (2015) 128, 219–224 doi:10.1242/jcs.142463

although a robust and extended GFP–desmin IF lattice was formed (Fig. 1G) in SW13 cell culture only when another IF protein such as vimentin (Fig. 1H) was present, there was no compensatory upregulation of vimentin observed in either desmin-null myotubes or desmin-null muscle fibers (data not shown).

The transfected muscle morphology also revealed a role for desmin in force transmission from the fiber exterior to the myofibrillar nuclei, based on the behavior of nuclei in single fibers. Nuclei in WT muscle subjected to stretch increased their length:width ratio (i.e. aspect ratio) in parallel with increased sarcomere length induced by stretch (Fig. 2A), whereas nuclei in desmin-null muscles were significantly less deformed by stretch (Fig. 2B). The deformation pattern of nuclei within desmin-null muscles transfected with GFP–desmin showed restored resting shape as well as restored deformation in response to stretch (Fig. 2C). Desmin-null muscles subjected to electroporation alone or transfection with GFP alone showed the same nuclear deformation pattern observed in untreated desmin-null muscles. This observation was confirmed quantitatively. Nuclear deformation was quantified by linear regression as the change in the normalized nuclear aspect ratio as a function of sarcomere length (Fig. 2D). The change in nuclear aspect ratio with sarcomere length was not significantly different between WT and GFP–desmin-transfected desmin-null muscles (Fig. 2E, $P>0.2$), but both were significantly greater than all control groups (Fig. 2E, $P<0.005$) demonstrating a rescued nuclear phenotype only in response to GFP–desmin transfection.

GFP–desmin transfection of desmin-null muscles also restored the normal mechanical response of the muscle to high stress. As we have shown previously (Sam et al., 2000), WT muscles subjected to high-stress eccentric contractions showed a significantly greater drop in isometric force compared to desmin-null muscles (Fig. 3A, WT versus No Tx, $P<0.0001$) (Sam et al., 2000). Importantly, in desmin-null muscles transfected with GFP–desmin, the magnitude of injury was significantly greater (i.e. significantly ‘more normal’) compared to untreated desmin-null muscles (Fig. 3A, $P<0.005$), desmin-null muscles transfected with a plasmid encoding GFP alone

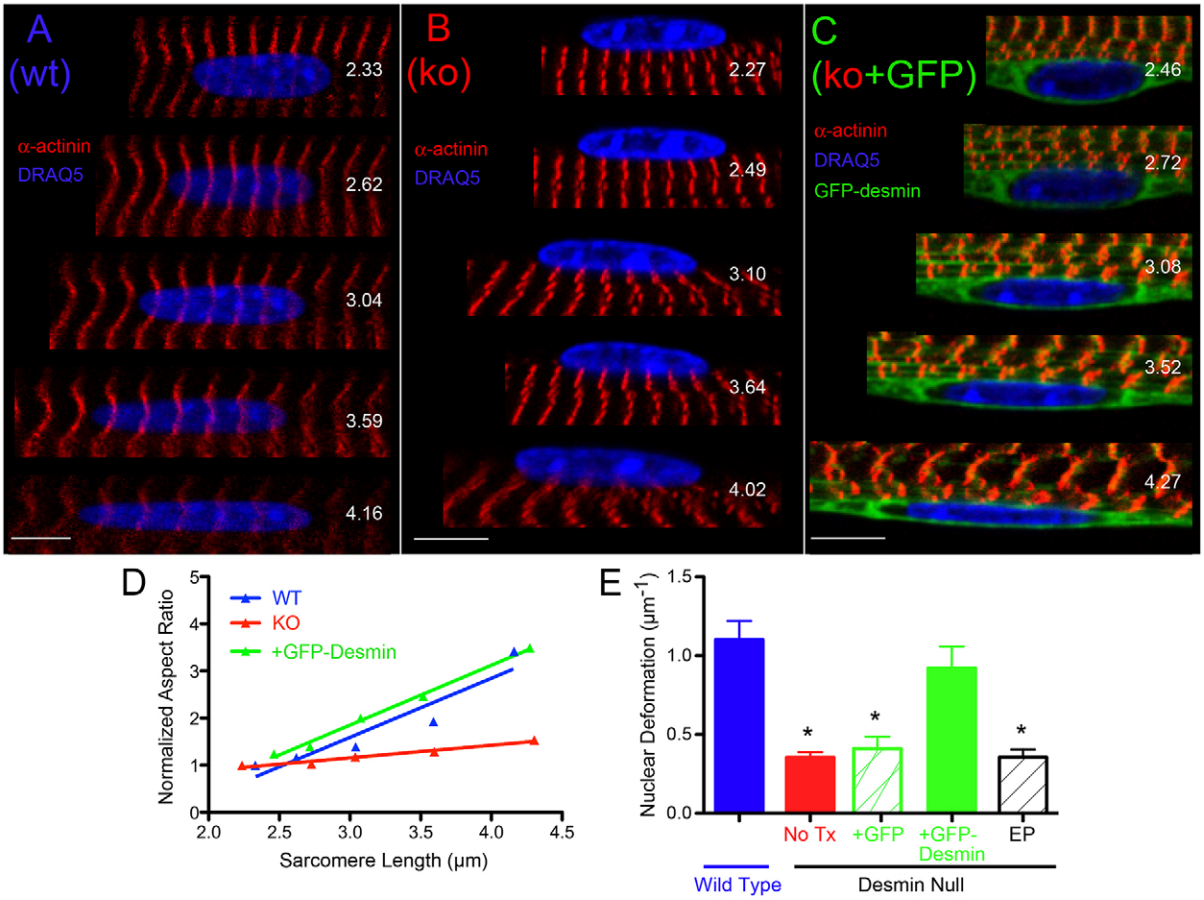

Fig. 2. Nuclear deformation pattern is rescued by transfection of desmin-null muscles with GFP–desmin. Serial confocal images of single myonuclei within a muscle cell being imaged while the cell is stretched. The nuclear aspect ratio is measured after each stretch. (A–C) Represent double labels of nuclei (shown in blue with DRAQ5) and striations (shown with α-actinin in red; GFP–desmin in is green) to obtain sarcomere length (shown in each image). The variable measured to quantify nuclear ‘deformability’ is change in aspect ratio as a function of sarcomere length (Shah et al., 2004). Values for change in normalized aspect ratio as a function of sarcomere length for each sample are: (A) WT nucleus, 1.25 μm^{-1}, (B) desmin-null nucleus, 0.268 μm^{-1}, (C) GFP-desmin transfected nucleus, 1.27 μm^{-1}. (D) Sample aspect ratio change data obtained from each of the experimental groups. Note the similarity in slopes between the WT (1.25 μm^{-1}) and the transfected desmin-null muscles (+GFP-desmin, (1.27 μm^{-1}) compared to desmin-null muscles (No Tx, 0.268 μm^{-1}). The curve for transfected desmin-null muscle has been displaced vertically by about 0.1 units for clarity. (E) Average normalized aspect ratio change for all specimens. Note that the change in aspect ratio for the GFP-desmin transfected desmin-null fibers is not significantly different from WT nuclei ($P>0.5$) but both are significantly different compared to the other three experimental groups *$P<0.001$ (Student’s *t*-test). Data represent mean±s.e.m., $n=15$–20 nuclei/muscle for $n=4$–6 muscles/group.

Journal of Cell Science (2015) 128, 219–224 doi:10.1242/jcs.142463

(Fig. 3A, $P<0.005$) or desmin-null muscles subjected to electroporation alone (Fig. 3A, $P<0.001$). Furthermore, a quantitative, nonlinear relationship was observed between muscle GFP–desmin content (Fig. 3B, inset), and the magnitude of injury after high stress contraction (Fig. 3B, green squares). The high nonlinearity of this relationship suggested a high degree of cooperativity within the myofibrillar matrix, perhaps reflecting regional influence of desmin across the muscle cell. To investigate this nonlinearity, desmin modulus values were estimated from AFM images and a finite element model of the

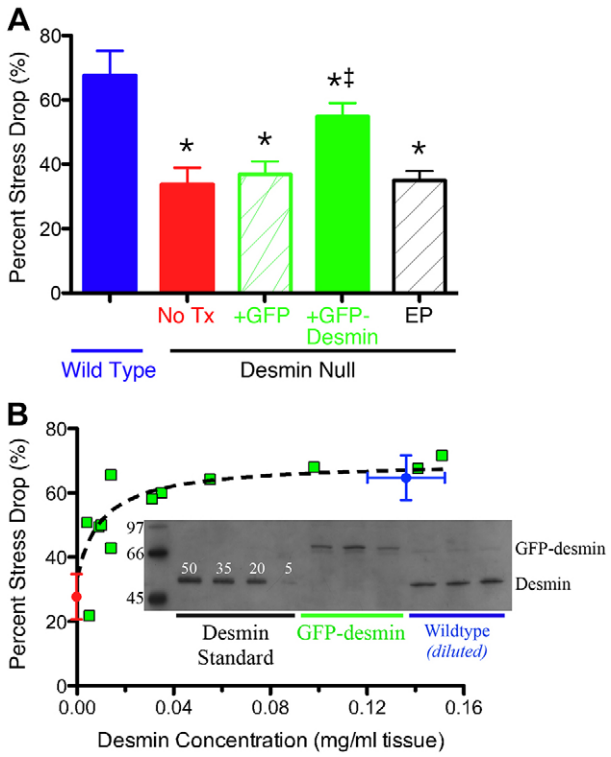

Fig. 3. Transfection of desmin-null muscle with GFP–desmin rescues mechanical function. As previously described, WT muscle demonstrates a larger percentage force drop compared to desmin-null muscles after high-stress contractions (Sam et al., 2000). (A) The measured decrease (in stress generation after high-stress contractions varies by genotype and treatment. A significant improvement in mechanical function is observed in the desmin-null muscles ($^{‡}P<0.05$ compared with the WT group) transfected with GFP–desmin (+GFP-Desmin) compared to any of the non-transfected groups (No Tx; red bar), desmin-null transfected with GFP (+GFP; green hatched bar), or desmin-null only electroporated (EP, black hatched bar), which show no significant difference from one another ($P>0.6$). *$P<0.05$, Student's *t*-test. Data represent mean±s.e.m., $n=4$–8 per group. (B) A dose-specific mechanical response is observed after transfection of desmin-null muscles with GFP–desmin. The relationship between the percentage decrease in stress generation among groups is shown as a function of desmin content. For desmin-null muscles (red symbol, desmin null), stress decrease is small (~35%) and desmin content is zero. For WT muscles (blue symbol, wild type), decrease in stress is relatively high (~65%) and desmin content is about 0.15 mg/ml tissue. For desmin-null muscles transfected with GFP–desmin (green squares), stress decrease varies nonlinearly with desmin content. This nonlinearity is well approximated by model predictions of desmin where preferential location is subsarcolemmal (black dashed line predicted as described in the Materials and Methods). Inset: western blots of GFP–desmin and desmin from WT muscles and GFP–desmin-transfected desmin-null muscles. Also shown are desmin standards used to quantify protein levels (linearity of calibration, $r^2=0.87\pm0.05$). Numbers to left of blot represent molecular mass standards. The data show the mean±s.e.m.

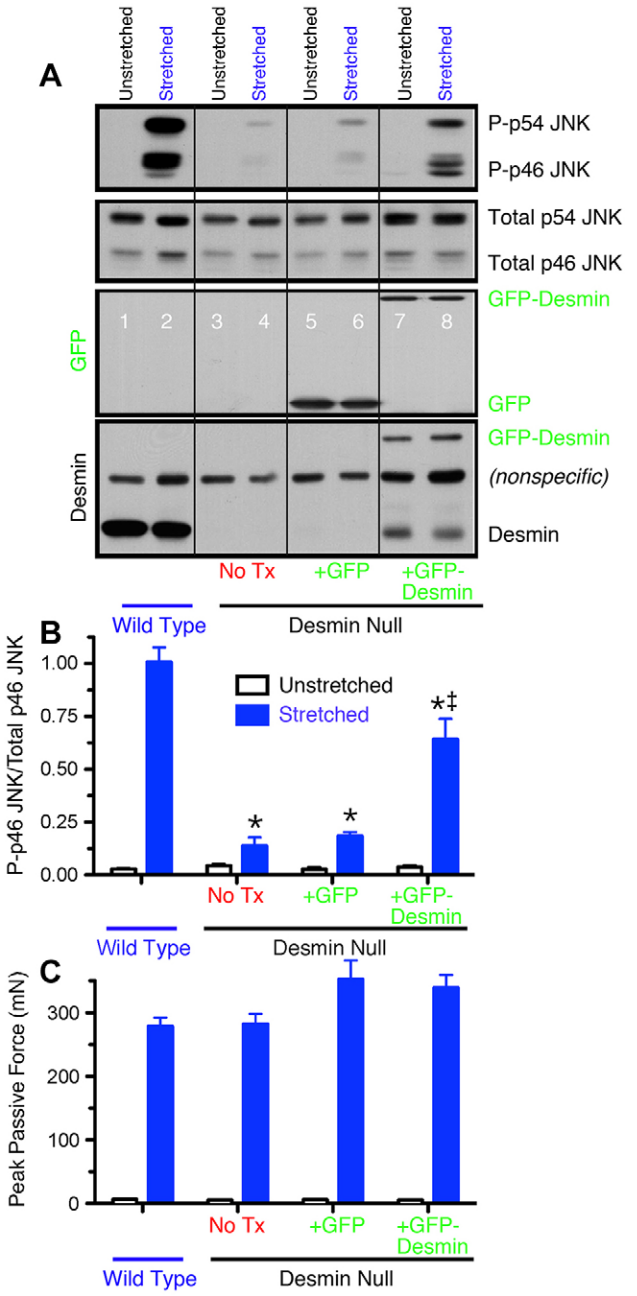

Fig. 4. GFP–desmin transfection rescues the normal JNK signaling response. (A) Western blots of p46 JNK and p54 JNK phosphorylation in stretched and unstretched extensor digitorum longus muscles. Antibodies used are, from top to bottom, phosphorylated JNK, total JNK, GFP and desmin. (B) Quantification of p46 JNK western blots, such as those shown in A. Note the strong phosphorylation of p46 JNK and p54 JNK upon stretch in WT muscles and desmin-null muscles transfected with GFP–desmin but not in untreated desmin-null muscles or desmin-null muscles transfected with GFP alone. Data shown are mean±s.e.m. ($n=4$ for each experiment). Also note that p46 JNK phosphorylation is partially rescued in desmin-null muscles transfected with GFP–desmin. Identical results were obtained for p54 JNK (data no shown). (C) Peak mechanical force reached during cyclic deformation of different treatment groups. No significant difference was observed between WT and desmin-null groups for any treatment demonstrating that the signaling difference was not simply a secondary effect of altered cellular mechanics. Data shown are mean±s.e.m. ($n=4$ for each experiment).

sarcomere matrix was generated based on known muscle fiber morphology, desmin tensile modulus and geometric sarcomere properties (Meyer et al., 2010). The sarcomere matrix was defined, and both passive and active viscoelastic forces were modeled to predict the force generated by the muscle as a function of desmin content as based on a previously defined linear relationship between muscle isometric stress and the percentage of force decline (Sam et al., 2000). The model predicted the observed nonlinear relationship between desmin content and force decline only when desmin was preferentially localized to the subsarcolemmal region (Fig. 3B, dashed line is the model prediction). When desmin was modeled as either being localized centrally within the fiber or randomly distributed across the fiber, less or no effect on force production was seen. The data and modeling strongly support a force-transmitting role for desmin and further suggest that the functional role of desmin might be region specific within the muscle cell.

Finally, the role of desmin in transducing cellular deformation was probed by stretching isolated muscles and measuring the degree of phosphorylation of the Jun N-terminal kinase (JNK; Hornberger et al., 2006). Stretch of WT muscle strongly phosphorylated both the 54 kDa and 46 kDa isoforms of JNK (most likely JNK2 and JNK1, respectively) (Fig. 4A, lanes 1 and 2; Fig. 4B). However, compared to WT muscle, desmin-null muscle showed a near absence of stretch-induced signaling leading to JNK phosphorylation (Fig. 4A, lanes 3 and 4; Fig. 4B), even though the peak stresses achieved during these stretches were not significantly different among these groups (Fig. 4C, $P>0.7$). Stress signaling to p46 and p54 JNK was partially rescued in desmin-null muscles transfected with GFP–desmin (Fig. 4A, lanes 7 and 8; Fig. 4B), providing further evidence that desmin plays a direct role in creating a stable IF network that can affect mechanotransduction and signaling within muscle.

Taken together, these data reveal a central role for desmin being involved in both mechanical stress transmission and stress transduction in muscle. We have demonstrated that desmin is specifically involved in myofibrillar alignment, nuclear integration within the myofibrillar matrix, mechanical response to high stress, and stress-mediated JNK signaling in muscle. These results illustrate that the Z-disk, and particularly its associated desmin cytoskeleton, play a central role in both muscle force transmission and signal transduction in muscle fibers. The molecular components of this interface remain to be determined, but it is clear that the muscle IF lattice plays a crucial role in converting mechanical forces into a biological response. This raises the possibility that IFs also play a similar role other cell types.

MATERIALS AND METHODS

Animal model

The animal model used was the desmin-knockout mouse previously reported (Li et al., 1997) and physiological experiments were performed on the 5th toe muscle of the extensor digitorum longus (EDL) (Chleboun et al., 1997). All animal experiments were performed according to approved guidelines.

Physiological testing

Eccentric contractions were imposed as previously described (Sam et al., 2000). Briefly, after excision, muscles were placed in Ringer's solution, equilibrated with a 95% O_2 and 5% CO_2. Maximum isometric tension was measured by applying a 400 ms train of 0.3 ms pulses delivered at 100 Hz while muscle length was held constant. Each muscle then underwent a series of 10 eccentric contractions, one every three minutes, in order to minimize the effects of fatigue. For each eccentric contraction, the muscle was first activated isometrically until tension stabilized (~200 ms), then a 15% fiber length (L_f) change was imposed at a rate of 2 L_f/s. This process was repeated ten times and isometric tension remeasured.

Muscle transfection

Plasmid DNA encoding a GFP–desmin chimeric protein was introduced into WT adult mouse muscle by electroporation (Vitadello et al., 1994). Expression of this protein *in vitro* resulted in GFP–desmin filaments from which the bending modulus could be calculated (Meyer et al., 2010) and which, *in vivo*, yielded a punctate appearance in the 20–80% of muscle fibers that were transfected. This morphology was in contrast to the results seen with a GFP-only construct whose gene product was diffusely distributed along the muscle fiber. Expression in adult muscle *in vivo* was transient, peaking 7 days after transfection and becoming significantly reduced after 28 days. Experiments reported here were thus performed on muscles 7 days after transfection at which time sufficient expression permitted both confocal imaging of GFP–desmin localization as well as evaluation of physiological function.

Single-cell imaging

Single fibers microdissected from wild type (WT) and either untreated, or transfected desmin-null muscles were subjected to confocal imaging during linear deformation to quantify the degree of sarcomere alignment, nuclear deformation and mechanical continuity under loading (Shah and Lieber, 2003; Shah et al., 2004).

Cell culture

Cell culture transfection experiments were implemented to investigate GFP–desmin filament formation in the presence and absence of vimentin. The SW13 cell line is an adrenal carcinoma line that is composed of a mixture of cells, none of which express desmin and about 80% of which express vimentin. Thus, we probed GFP–desmin polymerization in cell culture in the absence of desmin and in the presence of vimentin.

Antibodies

Confocal and western analysis used antibodies against vimentin [Cell Signaling; Vimentin (Red) Alexa 555-conjugated, product #9855], nuclear counterstaining with DRAQ5 [Cell Signaling (Far-Red) DNA-dye, product #4084] and α-actinin (Sarcomeric clone EA-53, Sigma-Aldrich, product #A7811).

Western blotting

Western blots were performed as previously described (Barash et al., 2002). Briefly, samples were extracted on ice in 100 µl SDS-PAGE sample buffer for at least 30 min, and then boiled for two min. 5 µl of a 1:3 dilution of each sample was loaded onto the gel, along with two lanes of desmin standards on opposite sides of the gel (catalog #RDI-PRO62005, Research Diagnostics, Flanders, NJ) and discontinuous SDS-PAGE was performed with acrylamide concentrations of 4% and 14% in the stacking and resolving gels, respectively. Gels were run at a constant current of 20 mA for 2.5 h at 4℃. Protein was transferred onto a nitrocellulose membrane (Bio-Rad) for 1 h at 100 V at 4℃. Blots were incubated with monoclonal antibodies against desmin (NCL-DER11) overnight at 4℃. The secondary antibody was peroxidase-labeled anti-mouse IgG antibody (Vector Laboratories). Bands were detected using enhanced chemiluminescence (ECL; Amersham Pharmacia Biotech, Piscatawy, NJ).

Finite element modeling

Sarcomeres were modeled as a repeating array of viscoelastic elements connected laterally by linear spring elements representing the contribution of desmin using a modification of our previous model (Meyer et al., 2010).

Fixed-end active fiber stress was predicted for ten different 'concentrations' of desmin ranging from zero (desmin$^{-/-}$) to a desmin element connecting every sarcomere laterally to its neighbors (wild type). For intermediate concentrations, we tested the effect of desmin

localization spring elements preferentially localized near the ECM, distributed randomly or preferentially localized away from the ECM.

Because muscle stress production scales linearly with the magnitude of injury experienced by the muscle (Sam et al., 2000), we predict the dependence of injury on desmin concentration. The predicted fit based on randomly distributed desmin links provided the best fit of the experimental measurements presented in Fig. 4B ($r^2=0.55$, $P<0.01$).

Acknowledgements

We thank J. Chen, V. Fowler, and S. Ward for critical discussions regarding this work. D. Hannaman and Ichor Medical Systems, Inc. provided assistance with the electroporation method. Semie Capetanaki generously provided the original desmin knockout breeders. We thank Sharon A. Huang for technical assistance.

Competing interests

The authors declare no competing interests.

Author contributions

M.G.P. and S.N.B. performed the electroporation, physiological and confocal microscopy experiments, T.A.H. performed the signaling experiments, G.A.M. performed the mathematical modeling, S.N.B. and S.B.S. performed the confocal microscopy experiments, B.K. and M.K. performed the atomic force microscopy, A.A.D. performed the SW13 cell transfection experiments, A.F.R. and R.L.L. designed the study, analyzed the data and wrote the paper. All authors discussed the results and edited the manuscript.

Funding

R.L.L. and coworkers are supported by the National Institutes of Health [grant numbers R01AR40050, P30AR061303]; and the Department of Veterans Affairs. Deposited in PMC for release after 12 months.

References

Barash, I. A., Peters, D., Fridén, J., Lutz, G. J. and Lieber, R. L. (2002). Desmin cytoskeletal modifications after a bout of eccentric exercise in the rat. *Am. J. Physiol.* **283**, R958-R963.

Buxboim, A., Ivanovska, I. L. and Discher, D. E. (2010). Matrix elasticity, cytoskeletal forces and physics of the nucleus: how deeply do cells 'feel' outside and in? *J. Cell Sci.* **123**, 297-308.

Chleboun, G. S., Patel, T. J. and Lieber, R. L. (1997). Skeletal muscle architecture and fiber-type distribution with the multiple bellies of the mouse extensor digitorum longus muscle. *Acta Anat. (Basel)* **159**, 147-154.

Engler, A. J., Sen, S., Sweeney, H. L. and Discher, D. E. (2006). Matrix elasticity directs stem cell lineage specification. *Cell* **126**, 677-689.

Frangos, J. A., McIntire, L. V. and Eskin, S. G. (1988). Shear stress induced stimulation of mammalian cell metabolism. *Biotechnol. Bioeng.* **32**, 1053-1060.

Fuchs, E. and Cleveland, D. W. (1998). A structural scaffolding of intermediate filaments in health and disease. *Science* **279**, 514-519.

Guharay, F. and Sachs, F. (1984). Stretch-activated single ion channel currents in tissue-cultured embryonic chick skeletal muscle. *J. Physiol.* **352**, 685-701.

Herrmann, H., Bär, H., Kreplak, L., Strelkov, S. V. and Aebi, U. (2007). Intermediate filaments: from cell architecture to nanomechanics. *Nat. Rev. Mol. Cell Biol.* **8**, 562-573.

Hornberger, T. A., Chu, W. K., Mak, Y. W., Hsiung, J. W., Huang, S. A. and Chien, S. (2006). The role of phospholipase D and phosphatidic acid in the mechanical activation of mTOR signaling in skeletal muscle. *Proc. Natl. Acad. Sci. USA* **103**, 4741-4746.

Lazarides, E. (1980). Intermediate filaments as mechanical integrators of cellular space. *Nature* **283**, 249-255.

Li, Z., Mericskay, M., Agbulut, O., Butler-Browne, G., Carlsson, L., Thornell, L. E., Babinet, C. and Paulin, D. (1997). Desmin is essential for the tensile strength and integrity of myofibrils but not for myogenic commitment, differentiation, and fusion of skeletal muscle. *J. Cell Biol.* **139**, 129-144.

Maniotis, A. J., Chen, C. S. and Ingber, D. E. (1997). Demonstration of mechanical connections between integrins, cytoskeletal filaments, and nucleoplasm that stabilize nuclear structure. *Proc. Natl. Acad. Sci. USA* **94**, 849-854.

Meyer, G. A., Kiss, B., Ward, S. R., Morgan, D. L., Kellermayer, M. S. Z. and Lieber, R. L. (2010). Theoretical predictions of the effects of force transmission by desmin on intersarcomere dynamics. *Biophys. J.* **98**, 258-266.

Milner, D. J., Mavroidis, M., Weisleder, N. and Capetanaki, Y. (2000). Desmin cytoskeleton linked to muscle mitochondrial distribution and respiratory function. *J. Cell Biol.* **150**, 1283-1298.

Morgan, D. L. (1990). New insights into the behavior of muscle during active lengthening. *Biophys. J.* **57**, 209-221.

Rudnicki, M. A., Schnegelsberg, P. N., Stead, R. H., Braun, T., Arnold, H. H. and Jaenisch, R. (1993). MyoD or Myf-5 is required for the formation of skeletal muscle. *Cell* **75**, 1351-1359.

Ruoslahti, E. and Pierschbacher, M. D. (1987). New perspectives in cell adhesion: RGD and integrins. *Science* **238**, 491-497.

Sam, M., Shah, S., Fridén, J., Milner, D. J., Capetanaki, Y. and Lieber, R. L. (2000). Desmin knockout muscles generate lower stress and are less vulnerable to injury compared with wild-type muscles. *Am. J. Physiol.* **279**, C1116-C1122.

Sawada, Y., Tamada, M., Dubin-Thaler, B. J., Cherniavskaya, O., Sakai, R., Tanaka, S. and Sheetz, M. P. (2006). Force sensing by mechanical extension of the Src family kinase substrate p130Cas. *Cell* **127**, 1015-1026.

Shah, S. and Lieber, R. L. (2003). Real-time imaging and mechanical measurement of muscle cytoskeletal proteins. *J. Histochem. Cytochem.* **51**, 19-29.

Shah, S. B., Davis, J., Weisleder, N., Kostavassili, I., McCulloch, A. D., Ralston, E., Capetanaki, Y. and Lieber, R. L. (2004). Structural and functional roles of desmin in mouse skeletal muscle during passive deformation. *Biophys. J.* **86**, 2993-3008.

Traub, P. and Shoeman, R. L. (1994). Intermediate filament proteins: cytoskeletal elements with gene-regulatory function? *Int. Rev. Cytol.* **154**, 1-103.

Vitadello, M., Schiaffino, M. V., Picard, A., Scarpa, M. and Schiaffino, S. (1994). Gene transfer in regenerating muscle. *Hum. Gene Ther.* **5**, 11-18.

Wang, K. and Ramirez-Mitchell, R. (1983). A network of transverse and longitudinal intermediate filaments is associated with sarcomeres of adult vertebrate skeletal muscle. *J. Cell Biol.* **96**, 562-570.